Analysis of HPVC Hub and Drivetrain

Abe Stucky

Sinjon Bartel

Leo Hill

John Carnprobst

February 2, 2018

Introduction

The following report documents the forces, stresses, and failure modes of each component in the Pitt Human Powered Vehicle Club custom front wheel drivetrain, seen in Figure 1 below.

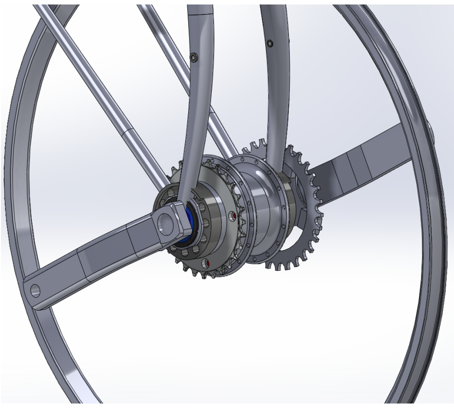

Figure 1: Isometric view of the drivetrain

Taking a look at the cross section (Figure 2), the hub assembly is broken down into four shafts: the hub, sleeve, bottom bracket shell, and crank shaft.

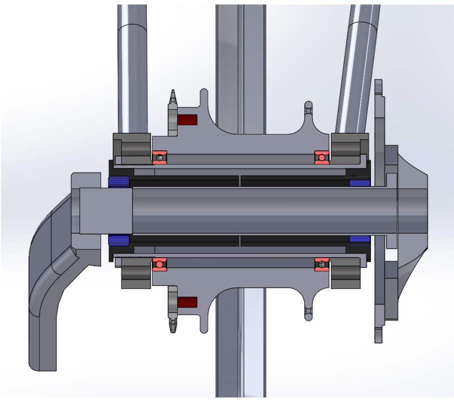

Figure 2: Cross section of hub

1 Reaction Force at Front Wheel

To start, we must determine the upwards reaction force at the location of the front hub from the weight of a 180 lb rider and weight of the bike (about 30 lbs). This totals to 210 lbf or 934 N. The bike is in static equilibrium, so the sum of the forces is 0 (Figure 3).

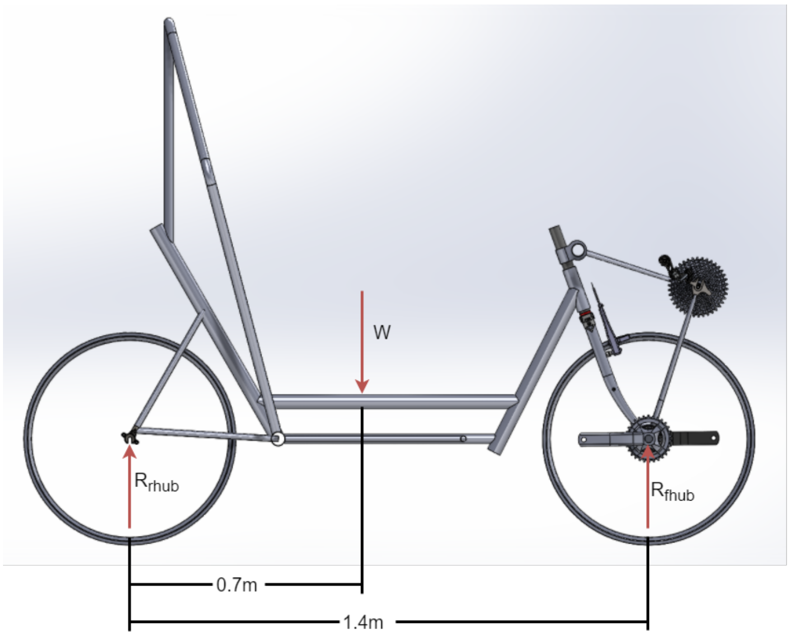

Figure 3: Free body diagram of the entire vehicle

$$\sum F_y \quad = 0 = R_{rearhub} + R_{fronthub} - 934N$$

$$\sum M_{rearhub} \quad = 0 = R_{fronthub}(1.4m) - 934N(0.7m)$$

$$R_{fronthub} = R_{rearhub} = 467N$$

2 Hub Analysis

The hub is a rotating enclosure which connects the drivetrain to the surrounding wheel. The hub features mounting points through which spokes may be laced; the combination of hub, spokes, and rim make a complete wheel. Placing a bottom bracket through a hub led to some nontraditional wheel building techniques; most notably, the spokes on the drive side of the wheel leave the hub at a steeper angle than do the spokes on the non-drive side. Paying careful attention during construction ensured the wheel to be properly dished and trued, so we believe wheel performance will not be affected by altered spoke pitch. We idealize the system by distributing the wheel's contact force equally among the four planar spoke mounting points.

Spoke tension and the tension present in the drive-side chain act on the body of the hub.

We begin our analysis by summing the forces in the x and y directions.

$$\sum F_y \quad = 0 = T_L + T_T + T_S(2\sin(\theta_L) + 2\sin(\theta_R) - R_{bL} - R_{bR}$$

$$\sum F_x \quad = 0 = T_S(\cos(\theta_L) + \cos(\theta_R)) - T_S(\cos(\theta_L) + \cos(\theta_R))$$

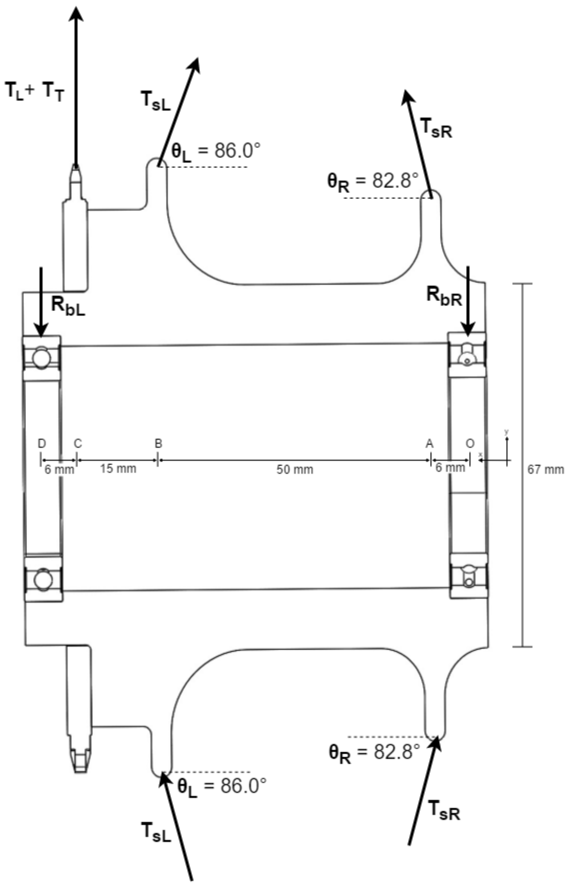

Figure 4: Free Body Diagram of hub forces

$$\sum M_O = 0 = (R_bL)(0.077) - (T_L + T_T)(0.071) - 2T_S(\cos(\theta_L) + \cos(\theta_R))(0.056) - 2T_S(\cos(\theta_L) + \cos(\theta_R))(0.006)$$

We assume the following values for the applied forces:

$$\mathrm{T_L} = 44.5 \text{ N}$$

$$\mathrm{T_T} = 435 \text{ N}$$

$$\mathrm{T_S} = 117 \text{ N}$$

With these loads, the hub bearings experience the following reaction forces:

$$\mathrm{R_{bL}} = 630 \text{ N}$$

$$\mathrm{R_{bR}} = 314 \text{ N}$$

This results in the hub experiencing the following shear forces and bending moments about its neutral axis:

As a result of the larger forces generated by pedaling, the greatest shear forces occur between the left bearing and the chainring. This results aligns well with our intuition about shaft loading.

The point along the axis in line with the left-side spoke flange experiences the greatest bending moment. We note this location and dedicate special attention to this region's increased potential for failure.

Measuring the chainring diameter as 60 mm, we assume a rider is capable of providing a constant torque and so we are able to calculate the torsional forces experience along crankshaft:

$$T = (T_T - T_l) \cdot (0.030)$$

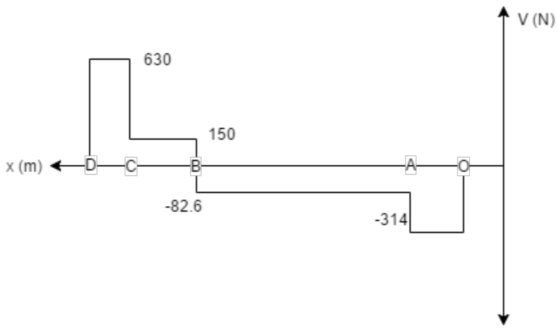

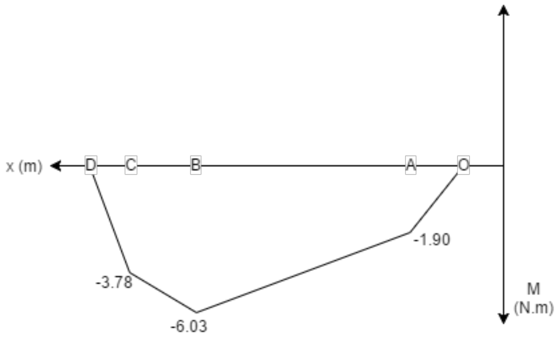

Figure 5: Hub Shear and Moment Diagrams

$$T = 11.7 N \cdot m$$

We observe the following mean and alternating values for maximum bending moment and torque at the previously identified area of interest:

$$\mathrm{M_a} = 6.03\ \mathrm{N \cdot m} \qquad \mathrm{T_a} = 0$$
$$\mathrm{M_m} = 0 \qquad \mathrm{T_m} = 11.7\ \mathrm{N \cdot m}$$

The maximum stresses due to the bending moments are alternating because of the nature of the pedaling action from the rider. Below summarizes the phenomena we will consider for fatigue analysis.

$$\sigma_a = \frac{M_a c}{I} \qquad \tau_a = \frac{T_a c}{J}$$

$$\sigma_m = \frac{M_m c}{I} \qquad \tau_m = \frac{T_m c}{J}$$

At this point, an appropriate failure criterion would be selected to compute whether or not this part achieves infinite life.

Complete analysis of the hub requires special attention be paid to areas with stress concentrations. We identified the **flange fillets**, **bearing shoulders**, and **spoke holes** as the primary stress concentrating regions.

One can conclude from this analysis that the hub is most likely to fail along the non-drive side spoke flange (Point B). In addition to being the location of a large stress concentrator, this region experiences the greatest alternating bending stress and the peak constant torsional stress. The expected mode of failure is ductile fracture due to fatigue by cyclic stress.

3 Sleeve Analysis

The sleeve lies within the hub between it and the bottom bracket shell. It is a hollow, circular shaft that is threaded on one end which can be tightened to keep it from sliding out. The sleeve experiences forces from the dropouts and bearings from the hub which are supported where the sleeve rests on the bottom bracket. The sleeve also experiences axial tension from being press-fit near the dropouts. This is shown on the free body diagram below, however the axial tension is expected to be small, and therefore the results from the vertical forces will be the main consideration with respect to failure

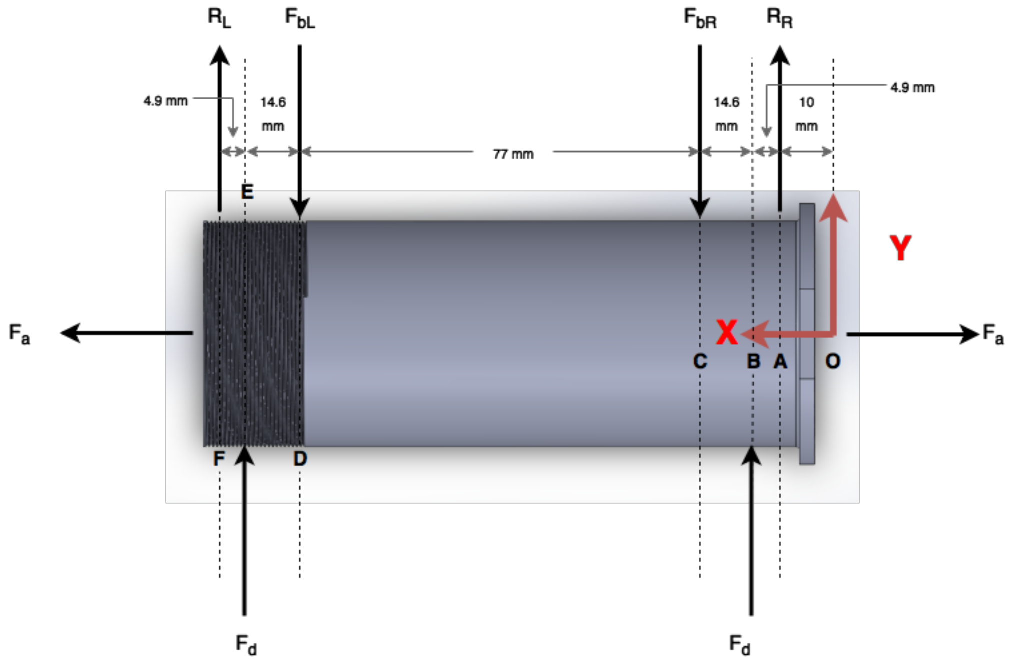

Figure 6: Free Body Diagram of the Sleeve

The origin is offset to the right of the diagram just to keep it consistent with the other component analyses. The first step is simple static analysis to solve for the reactionary forces generated by the contact between the sleeve and the bottom bracket. This will be done by summing the forces in the y-direction and the moments about the point A. The forces on the bearings below were carried over from the hub analysis above and the forces on the dropouts were determined from halving the force on each wheel, which was determined in the opening section.

$$F_{br} = 314N$$
$$F_{bl} = 630N$$
$$F_d = 233N$$

$$\sum M_A = 0 = F_{br}(0.0195) + F_{bl}(0.0965) - R_l(0.116) - F_d(0.0049 + 0.1111)$$

$$R_l = 343.9N$$

$$\sum F_y = 0 = R_r + R_l - F_{bl} - F_{br} + (2)F_d$$

$$R_r = 134N$$

Now that the forces are all solved for, a shear and moment diagram can be constructed to identify the critical stress points in the sleeve.

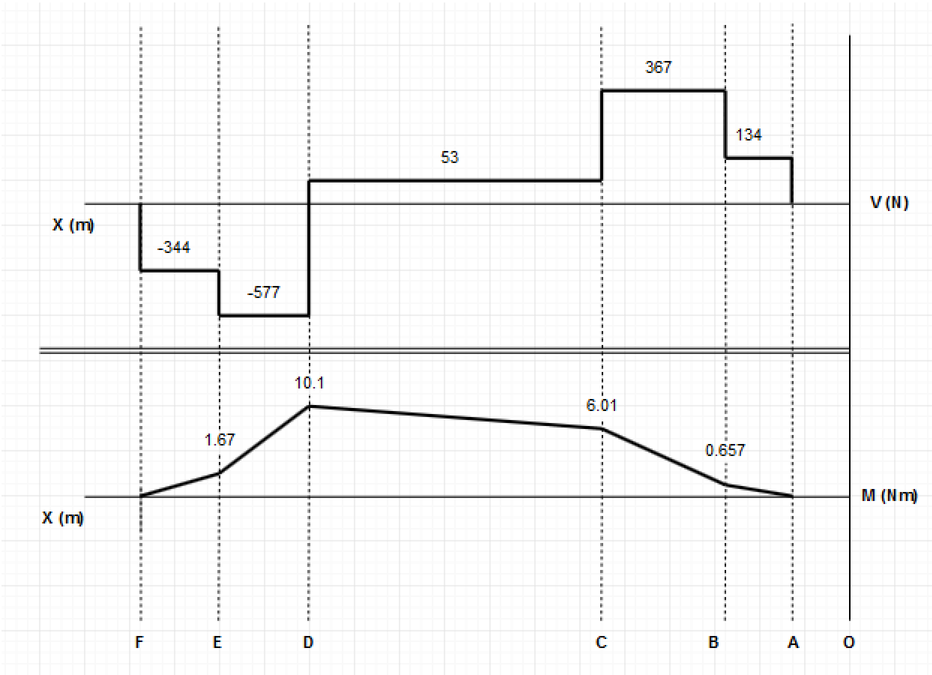

Figure 7: Shear and Moment Diagram for the Sleeve

As seen above, the greatest stress due to bending is located at point D, which is the contact point between the sleeve and the leftmost bearing on the hub. However, there is a relatively high bending moment in the full range between C and D. Therefore, the whole middle section should be further analyzed for possible failure modes. Also, the axial tension referred to earlier in this section will add to this issue, making the entire outer surface on the top half of the sleeve more susceptible to failure. It is recommended to use the maximum shear failure theory, as this is a conservative method. The principal stresses would be due to bending and axial tension, and it would be wise to build in a factor of safety as seen below.

$$\sigma_1 = \frac{M_{max}c}{I}$$

$$\sigma_2 = \frac{F_{max}}{A}$$

$$\frac{S_y}{n} = \sigma_1 > \sigma_2$$

The maximum stresses due to the bending moments are constant because the sleeve is not rotating, and there are no torques present on the sleeve. Below summarizes the phenomena used for fatigue analysis, but since there are not alternating stresses present, this will not be a concern with regard to failure.

$$\sigma_a = \frac{M_a c}{I} \qquad \tau_a = \frac{T_a c}{J}$$

$$\sigma_m = \frac{M_m c}{I} \qquad \tau_m = \frac{T_m c}{J}$$

where:

$$M_a = 0Nm \qquad T_a = 0Nm$$

$$M_m = 10.1Nm \qquad T_m = 0Nm$$

One improvement to this design would require including some sort of support in the open area between the two bearings in order to alleviate that large bending moment across that region. This way, the moment would not propagate over the length between C and D, capping the maximum moment somewhere around 6 Nm rather than 10 Nm.

Stress concentrations are present on the threaded end of the sleeve, specifically between points D and F. This stress concentration could be idealized as a continuous notch wrapping around the perimeter of the cylinder. The continuous notch would need further analysis beyond this point, however, because a continuous thread would be expected to behave slightly differently compared to a single notch. What is more concerning is the fact that the largest moment in the sleeve is compounded by the stress concentration (Point D). This is especially significant because point D is located at the beginning of the thread, which is where the stress flow lines will be most directly obstructed. A way to fix this could be to shorten the thread so that it does not reach point D. This sounds doable because the thread seems to serve no other purpose besides making sure the sleeve does not slide out.

One can conclude from this analysis that the point of failure in the sleeve will almost surely occur at point D barring unforeseen circumstances. This failure could occur in the form of plain ductile yielding, or a crack could propagate at point D at the root of the thread due to the stress flow lines being abruptly obstructed. Either way, further analysis should be done on this section of the sleeve in order to fully understand the risk for failure and potentially retire this risk in other ways besides the ones mentioned above.

4 Bottom Bracket Shell Analysis

The PF41 bottom bracket encompasses two machined plastic or alloy cups, the “shell”, with two sealed bearings pressed in (see Figure).

Figure 8: Stock photo of a PF41 bottom bracket [Tak17]

Figure 9: Isometric Solidworks model of the bottom bracket

The female cup is sliding-fit tolerance as the male cup is threaded in and tightened down. This system effectively secures the bottom bracket to the frame - The exterior makes contact force with the sleeve, and the interior ball bearings interface with the crankshaft.

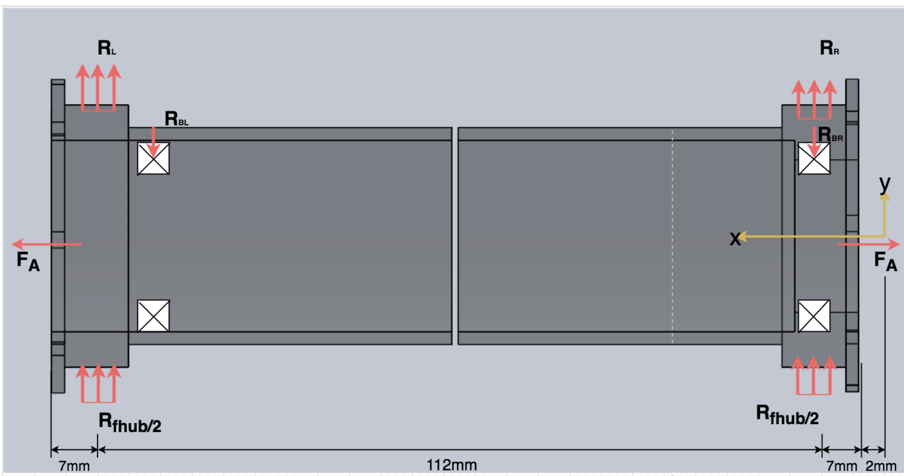

Figure 10: Free Body Diagram of the Bottom Bracket

The free body diagram of the bottom bracket in the x-y plane can be idealized as a beam, simply supported on each end (see Figure). We idealized the contact force from the sleeve as equally distributed among the contact points. The reaction forces are on the internal chromium steel ball bearings.

Analysis begins by summing the forces in the x and y directions:

$$\sum F_y = 0 = R_L + R_R + R_{fhub}/2 + R_{fhub}/2 - R_{bL} - R_{bR}$$

$$\sum F_x = 0 = F_{Ar} - F_{Al}$$

$$\sum M_O = 0 = -(R_L)(0.121) - (R_{fhub})(.121) + (R_{bL})(.119)$$

Assuming the following applied force as shown in Section 2:

$$R_{\text{fhub}} = 467 \text{ N}$$

With these loads the hub bearings experience the following reaction forces:

$$R_{\text{bL}} = 474.9 \text{ N} \qquad R_{\text{bR}} = 459.2 \text{ N}$$

A bending moment diagram is used to determine the location of the max bending moment:

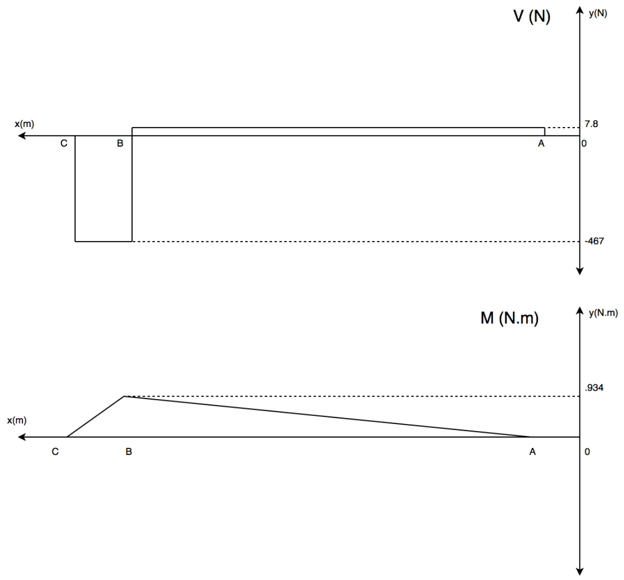

Figure 11: Bottom Bracket Shear and Moment Diagram

As a result, the greatest shear forces occur at the interface between the left bearing and the left contact point with the sleeve. The greatest bending moment occurs at the non-driveside bearing. This location should be noted for increased potential for failure from shear stress.

It is worth noting the following mean and alternating values for maximum bending moment and torque at the previously identified area of interest:

$$M_{alt} = 0N \cdot m \qquad T_{alt} = 0N \cdot m$$

$$M_{mean} = 0.934N \cdot m \qquad T_{mean} = 0N \cdot m$$

The shell is made from ductile aluminum, so the von Mises stress can be calculated and compared to yield stress of the material. Both the axial stress from tightening the male and female sections together and bending stress should be factored into this calculation.

5 Crank Shaft Analysis

The crankset encompasses two crank arms, a chainring, and a hollow shaft connecting the two crank arms (see figure).

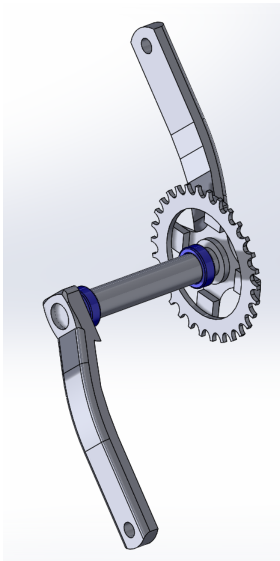

Figure 12: Crankset

As a rider pedals, they apply a force to each pedal and corresponding force couple (torque) to the crankshaft. Throughout the revolution of a pedal, the pedaling force varies with the position in the stroke, as shown by the figure.

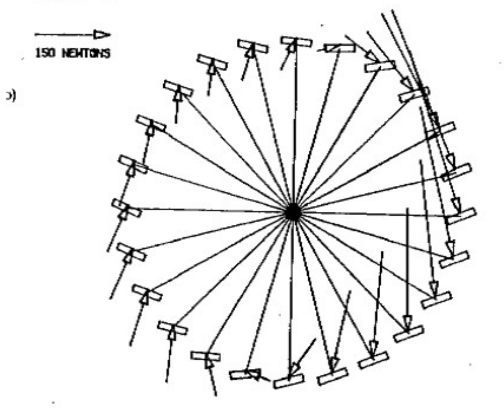

Figure 13: Free body diagram of forces acting on pedal throughout pedal stroke [Jim11]

At its peak, the max force acting on a pedal is around 150 N according to [Com11] but since the same forces are mirrored 180 degrees to the opposite pedal, the crankshaft was idealized to experience a constant torque with the rider pedaling at max speed. With a crank arm length of 170mm, the mean torque is expressed as

$$T = 150N(0.17m) = 25.5N \cdot m$$

Since the crankset is assumed to be in static equilibrium, $\sum T \ = 0$

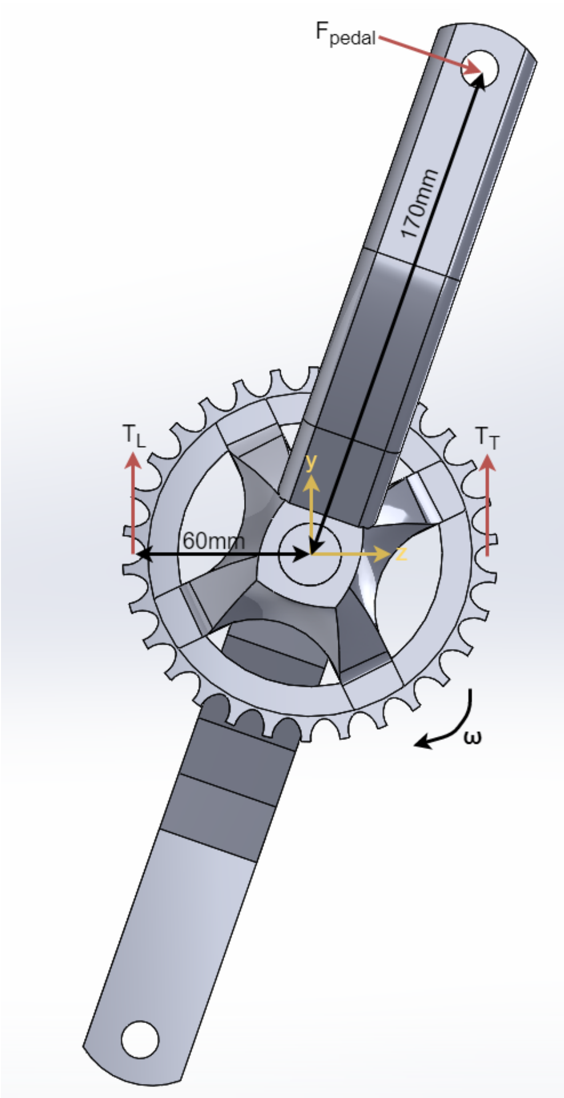

Figure 14: Free body diagram of torques

$$\sum T \ = 0 = -150N(0.17m) - 0.060m(13.3N) + T_{tight}(0.060m)$$

$$\sum M_{rearhub} \ = 0 = R_{fronthub}(1.4m) - 934N(0.7m)$$

$$T_{tight} = 438.3N$$
$$T_{loose} = 13.3N$$

The freebody diagram of the crankshaft can be idealized as a shaft on two pillow bearings with an attached chainring. Drawing a free body diagram on the XY plane:

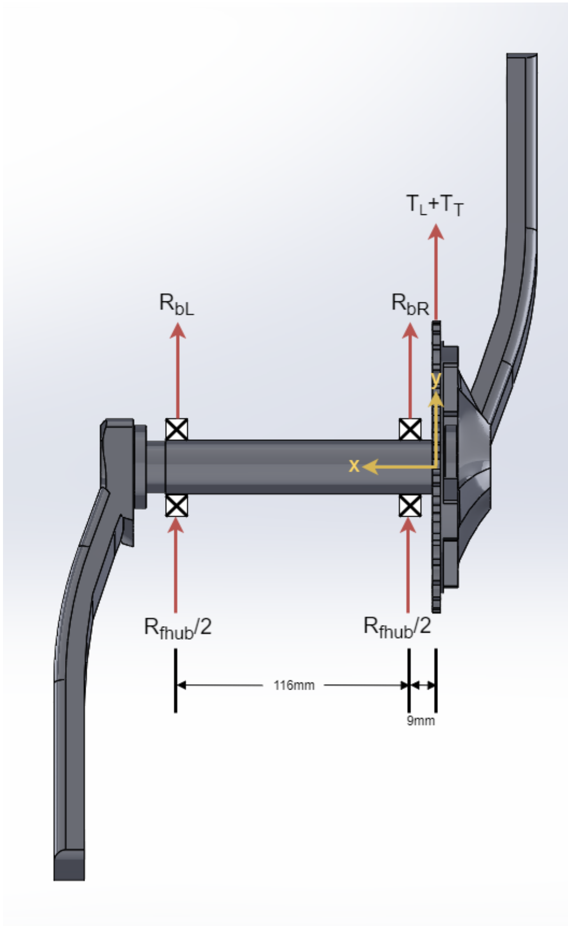

Figure 15: Free body diagram of forces acting on the crankset

Note that the reaction force on the front hub from the weight of the bicycle and rider is distributed between the two sealed bearings.

$$\sum F \ = 0 = 452N + R_{bL} + R_{bR} + \frac{467N}{2} + \frac{467N}{2}$$

$$\sum M_L \ = 0 = R_{bR}(0.116) + \frac{467N}{2}(0.116) + 452N(0.125)$$

$$R_{bR} = -721N$$

$$R_{bL} = -198N$$

Drawing the shear and bending moment diagrams

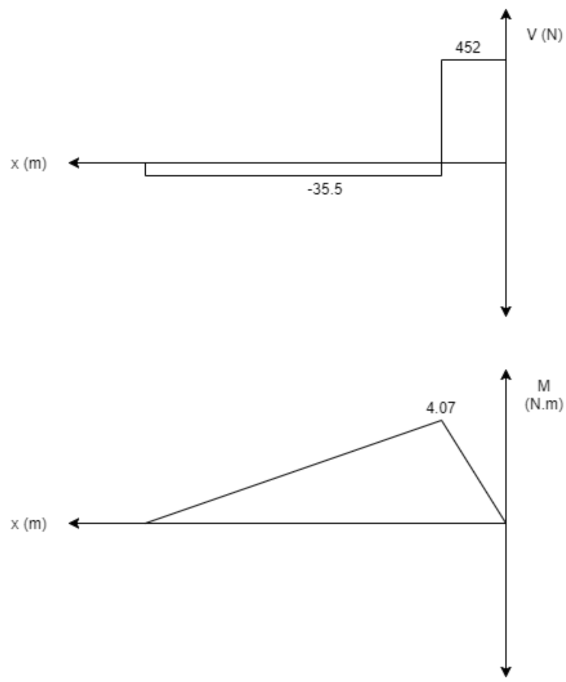

Figure 16: V-M diagram of the crankshaft

The max bending moment is 4.07 N·m and occurs at $x = 0.009m$ (driveside bearing). Looking at stress element on outside of shaft at $x = 0.009m$.

$$\sigma_{alt} = \frac{M_{alt} c}{I}$$

$$\tau_{xy} = \tau_{mean} = \frac{T_m c}{J}$$

In summary, there is an alternating bending stress from the alternating bending moment and a mean shear stress from the mean torque.

$$M_{alt} = 4.07 N \cdot m \qquad T_{alt} = 0$$

$$M_{mean} = 0 \qquad T_{mean} = 25.5 N \cdot m$$

The shaft is made from a ductile material (aluminum), so the Distortional Energy Theory can be used to find the equivalent mean and alternating stresses:

$$\sigma'_{alt} = \sqrt{\sigma_{alt}^2 + 3\tau_{alt}^2} = \sigma_{alt} \qquad \sigma'_{mean} = \sqrt{\sigma_{mean}^2 + 3\tau_{mean}^2} = \sqrt{3}\tau_{mean}$$

Next, apply a fatigue failure criterion such as the modified Goodman relationship

$$\frac{1}{n} = \frac{\sigma'_{alt}}{S_e} + \frac{\sigma'_{mean}}{S_{ut}}$$

Compare this n to the factor of safety guarding against static failure

$$n_y = \frac{S_y}{\sigma'_{max}}$$

Other modes of failure in the crankset include shear stress in the crank bolts that connect the chainring to the crankarm.

6 Conclusion

In summary, in the hub, the maximum moment was 6.03 N·m and the maximum torque was 11.7 N·m. The moment occurs at point B in Figure 4 and the torque is constant across the hub. The hub is most likely to fail along the non-drive side spoke flange (Point B) as a result of ductile fracture or cyclic fatigue. The sleeve experienced a maximum moment of 10.1 N·m and no torque. The maximum moment occurs at point D on Figure 6. The sleeve is most likely to fail at the contact point between the sleeve and the leftmost bearing on the hub (Point B) as a result of ductile yielding or crack propagation at the root of the thread. The bottom bracket shell experienced a maximum moment of 0.934 N·m and no torque. The maximum moment occurs at point B on Figure 11. The bottom bracket shell is most likely to fail at the non-driveside bearing in single or double shear. The crank shaft experiences a maximum moment of 4.07 N·m and a torque of 25.5 N·m. The maximum moment occurs at x = 0.009 m in Figure 15 and the maximum torque occurs across the entire crankshaft. The crank shaft is most likely to fail at the driveside bearing due to cyclic fatigue or shear stress in the crank bolts.

References

[Com11] Tom Compton. Forces on rider. *Analytic Cycling*, 2011.

[Jim11] Jim M. Papadopoulos. Pedal forces, 2011. [Online; accessed January 20, 2011.

[Tak17] TakeAHikeShop. Bottom bracket, 2017. [Online; accessed January 20, 201].